Neutron Imaging

Luise Theil Kuhn

(Head of Section Imaging and Structural Analysis)
luku@dtu.dk

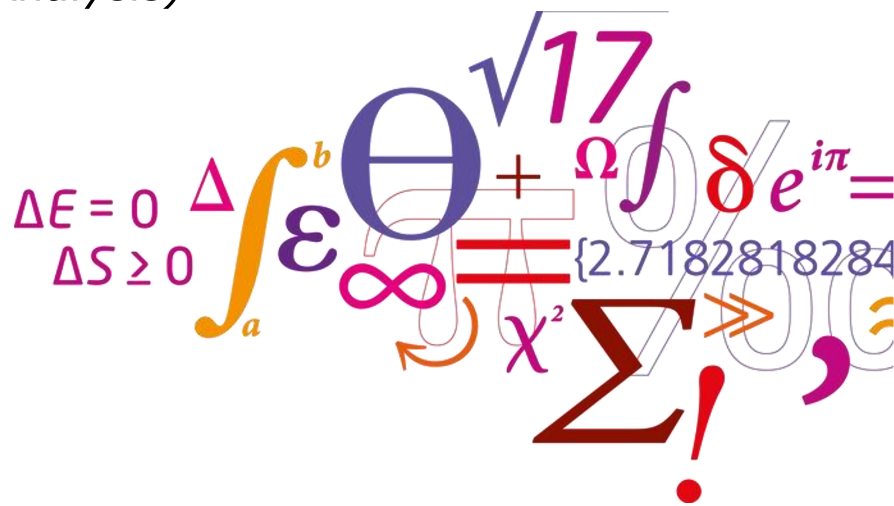

DTU Energy
Department of Energy Conversion and Storage

Motivation

This module's important concepts

- Instrumentation
- Radiography
- Tomography
- In operando
- Virtual Imaging experiment

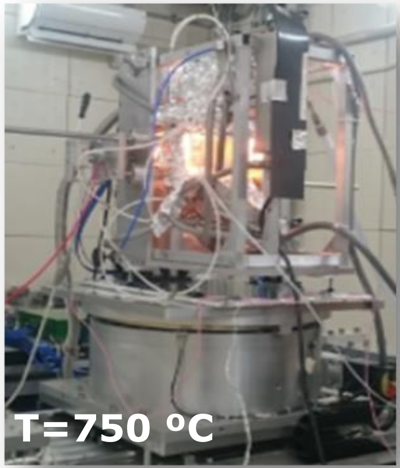

Learning objectives

A student who has successfully completed this module should be able to:

- Describe how the image and contrast is formed during neutron imaging and how it differs from X-ray imaging

- Explain the contributions to the neutron attenuation, and explain the relationship between the attenuation coefficient and the scattering cross section

- Explain the principles behind various types of neutron imaging methodologies

- Decide which combination of pinhole diameter, pinhole-sample distance, and sample-detector distance gives the best spatial resolution for a given experimental setup

Learning objectives

A student who has successfully completed this module should be able to:

- Decide which of the experimental parameters pinhole diameter, pinhole-sample distance, and sample-detector distance you should modify to reduce the blur at a given neutron flux and divergence

- Evaluate the quality of a tomographic reconstruction by applying the filtered backprojection algorithm

- Evaluate the advantages of neutron radiography compared to neutron tomography

- Give design principles for a neutron imaging setup for 2D and 3D analysis of a given type of sample

Image and contrast formation

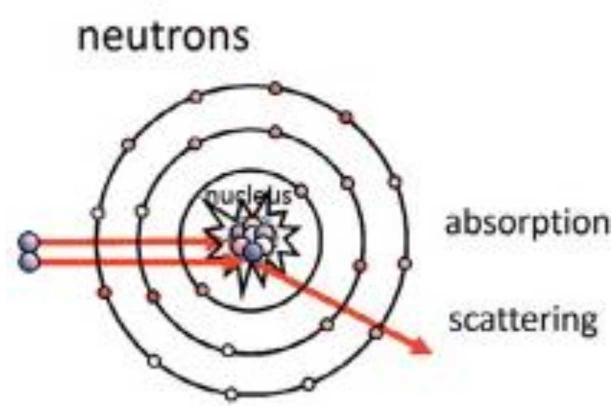

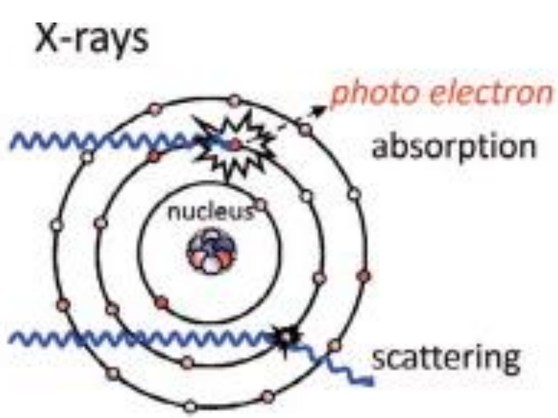

Image and contrast formation

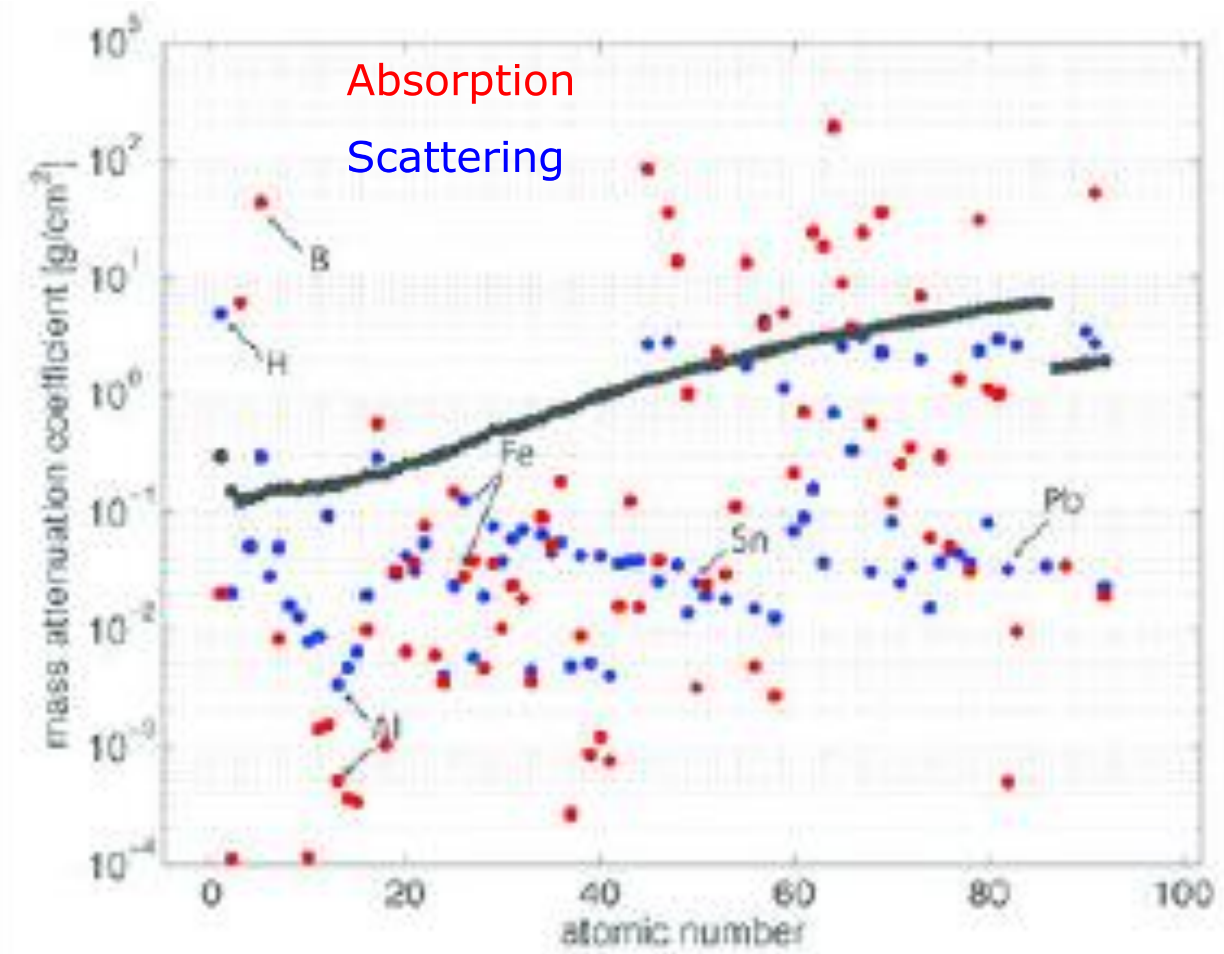

$$\frac{\mu}{\rho} = \frac{N_a}{M}\sigma$$

Radiography

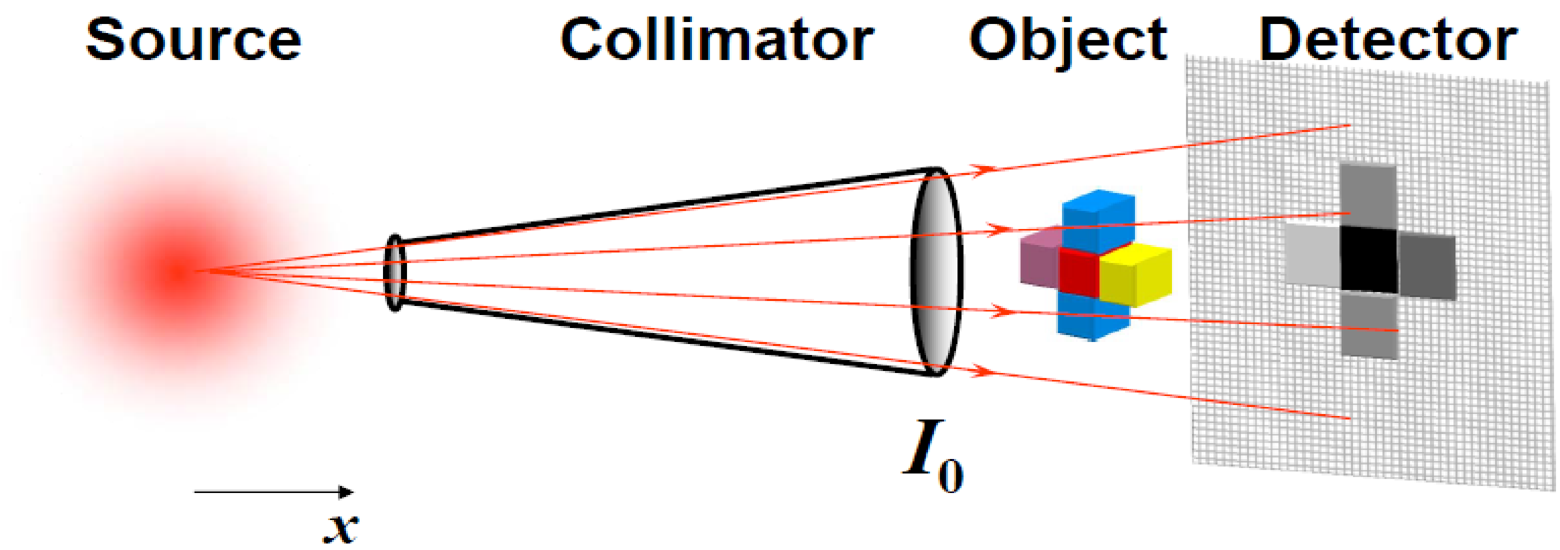

Beer-Lambert law: $\sim I_0 e^{-\int \mu(x)dx}$

x – propagation direction

I_0 – primary beam

$\mu(x)$ – attenuation coefficient

$\mu_{total} = \mu_a + \mu_s$

Strobl, M. et al. (2009). *J. Phys. D. Appl. Phys.* **42**, 243001.

Setup: ICON @ PSI

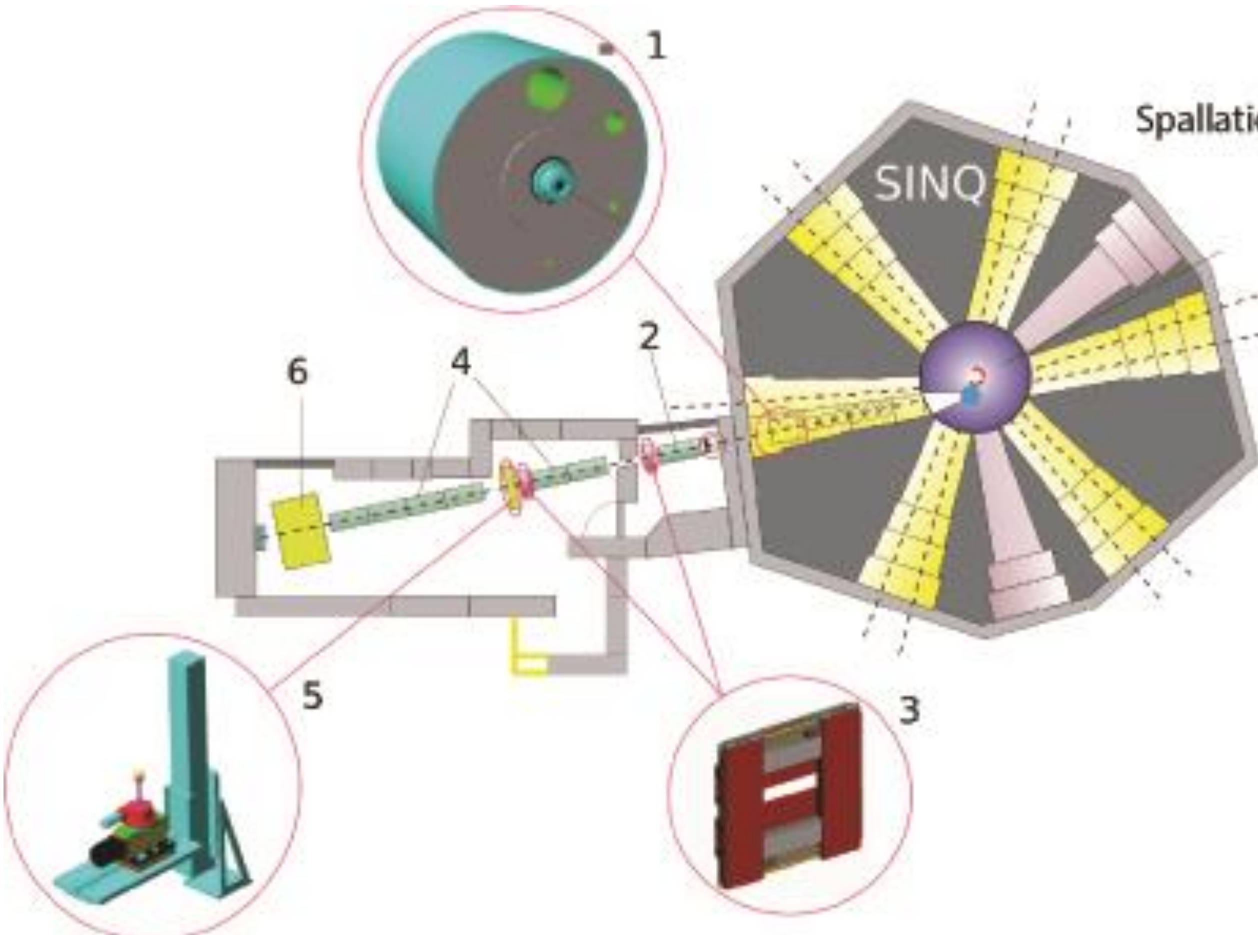

1. Pinhole
2. Flight tube
3. Beam limiters
4. Flight tube
5. Sample stage for small samples
6. Sample stage for large samples

Spatial resolution

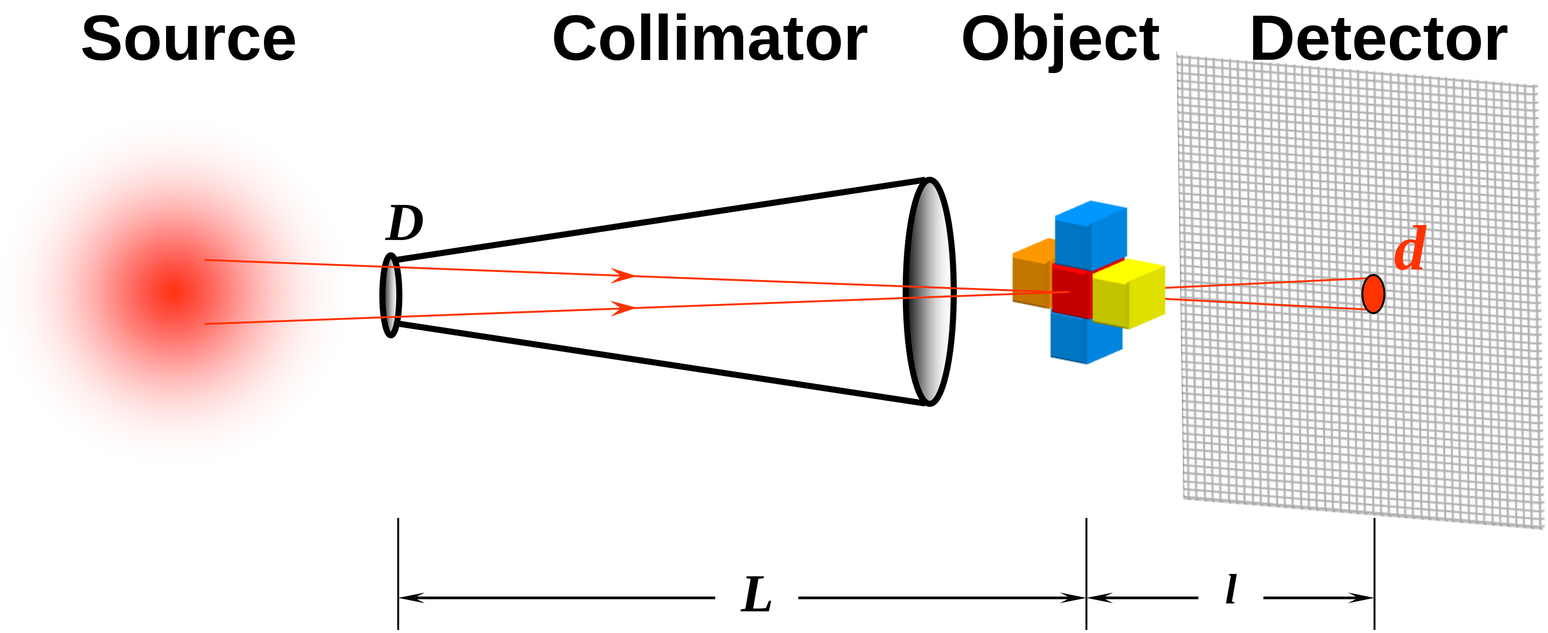

D – Collimator aperture, pinhole

L – Distance Collimator-Object

l – Distance Object-Detector

$$d = \frac{l}{L/D}$$

Strobl, M. et al. (2009). *J. Phys. D. Appl. Phys.* **42**, 243001.

Spatial resolution - Siemens star

32.9 μm

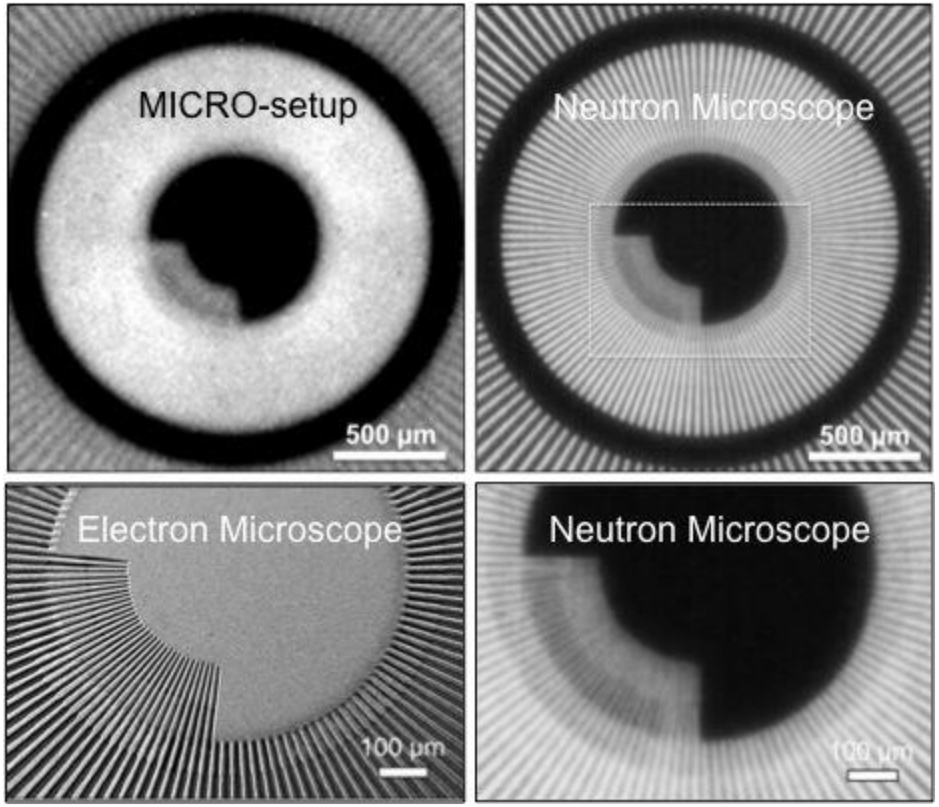

7.6 μm

Trtik, P. et al. (2015). *Physics Procedia.* **69**, 169.

Detectors

Charged Coupled Device

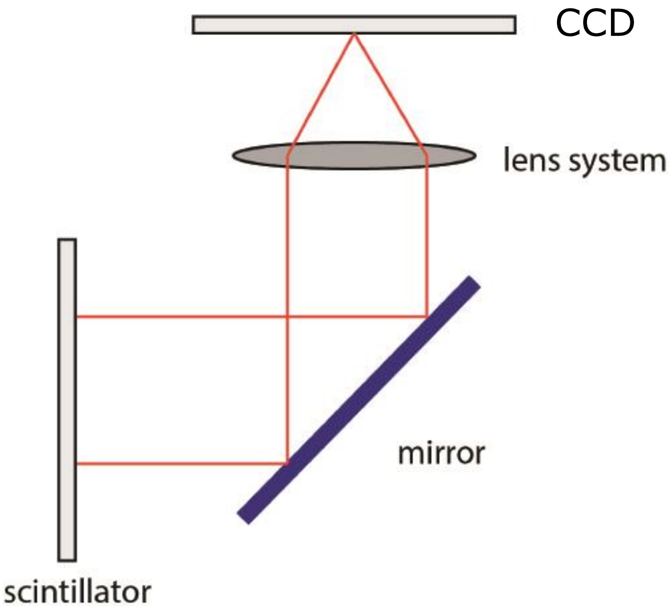

Multi Channel Plate

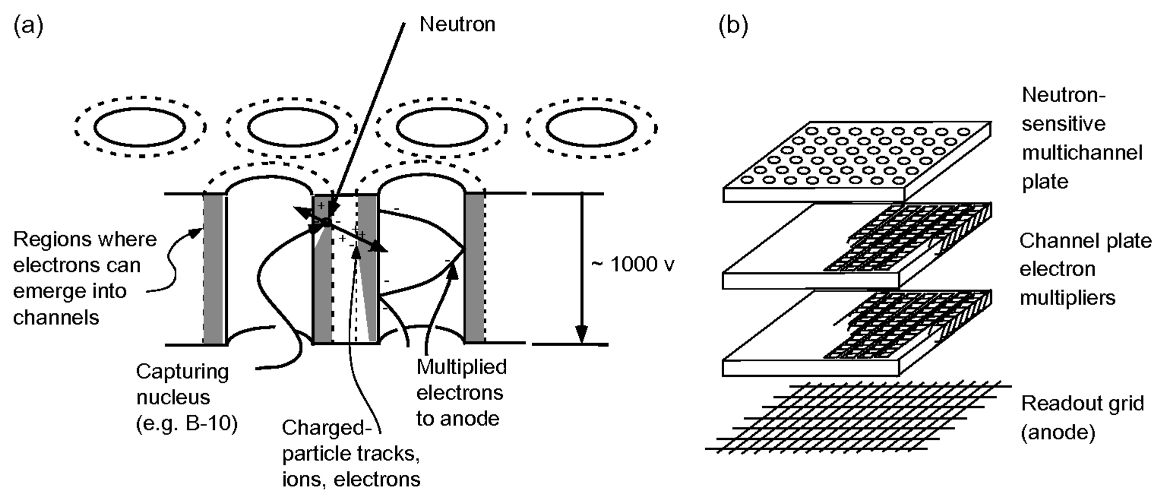

http://www.novascientific.com/technology/

Principle for data acquisition in imaging experiment

1. Raw image, I_θ
2. Dark field image (no beam), correct for dark-current in detector system, *DF*
3. Flat-field image (open beam), correct for inhomogeneities in beam-profile and in detector screen, *FF*
4. Image, T_θ

$$T_\theta = \frac{I_\theta - DF}{FF - DF}$$

Tomography

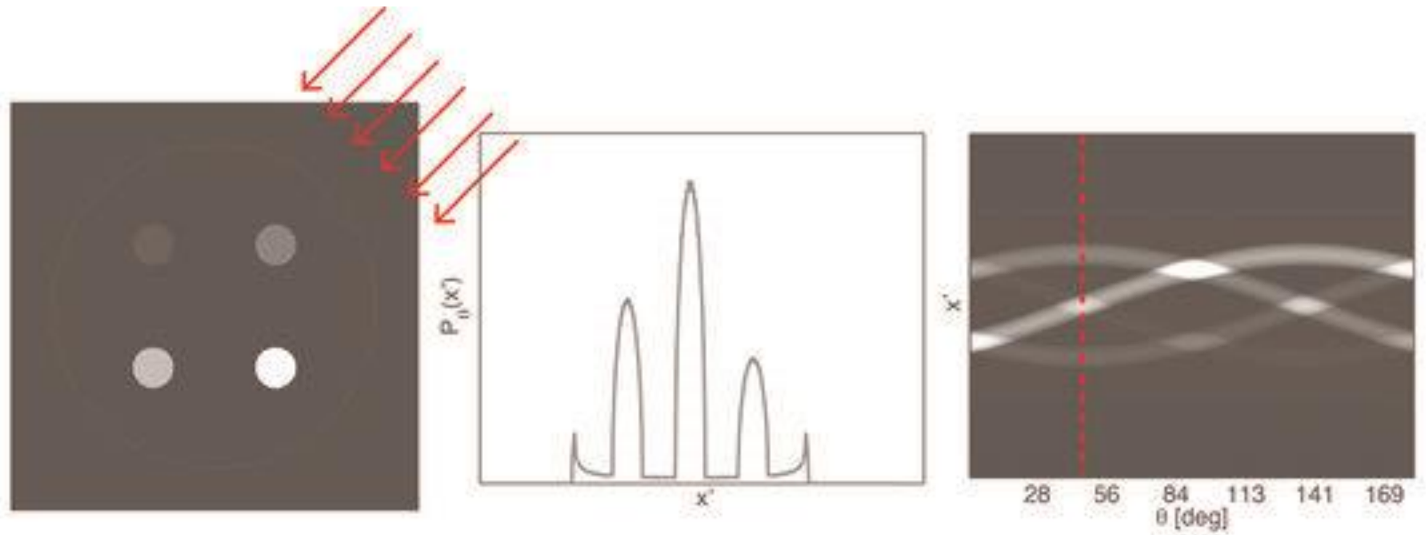

2D sample   Projection image T_θ Sinogram

Tomographic reconstruction

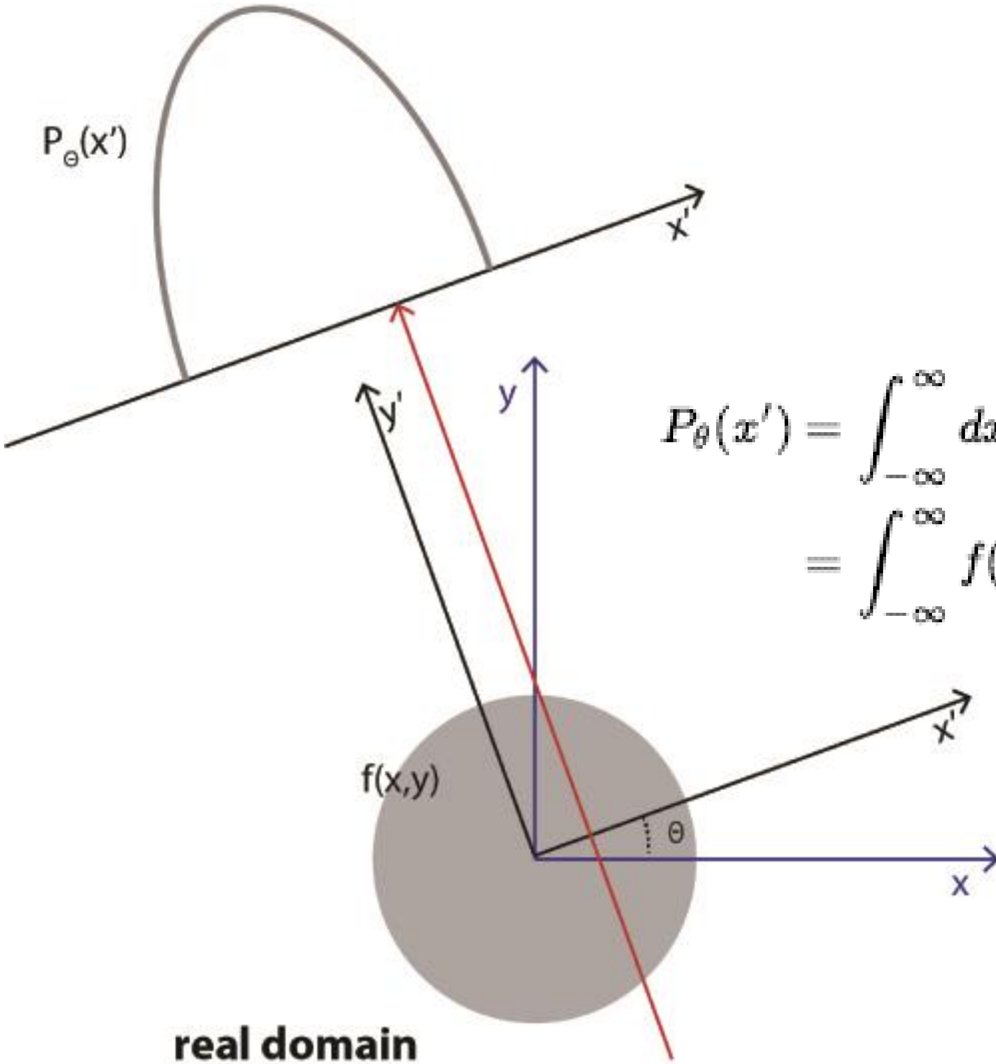

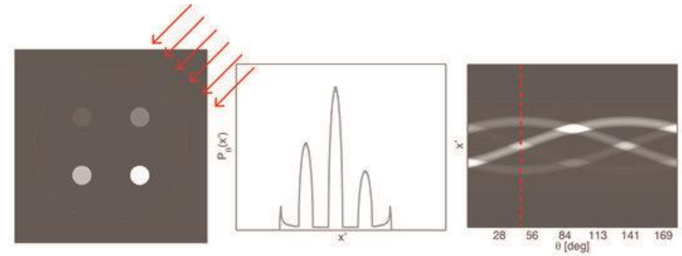

$$P_\theta(x') = \int_{-\infty}^{\infty} dx \int_{-\infty}^{\infty} dy f(x,y)\delta(x\cos(\theta) + y\sin(\theta) - x')$$
$$= \int_{-\infty}^{\infty} f(x', y')dy'$$

$$\begin{pmatrix} x' \\ y' \end{pmatrix} = \begin{bmatrix} \cos\theta & \sin\theta \\ -\sin\theta & \cos\theta \end{bmatrix} \begin{pmatrix} x \\ y \end{pmatrix}$$

$$P_\theta(x') = -\ln(T_\theta(x'))$$

Fourier Slice Theorem

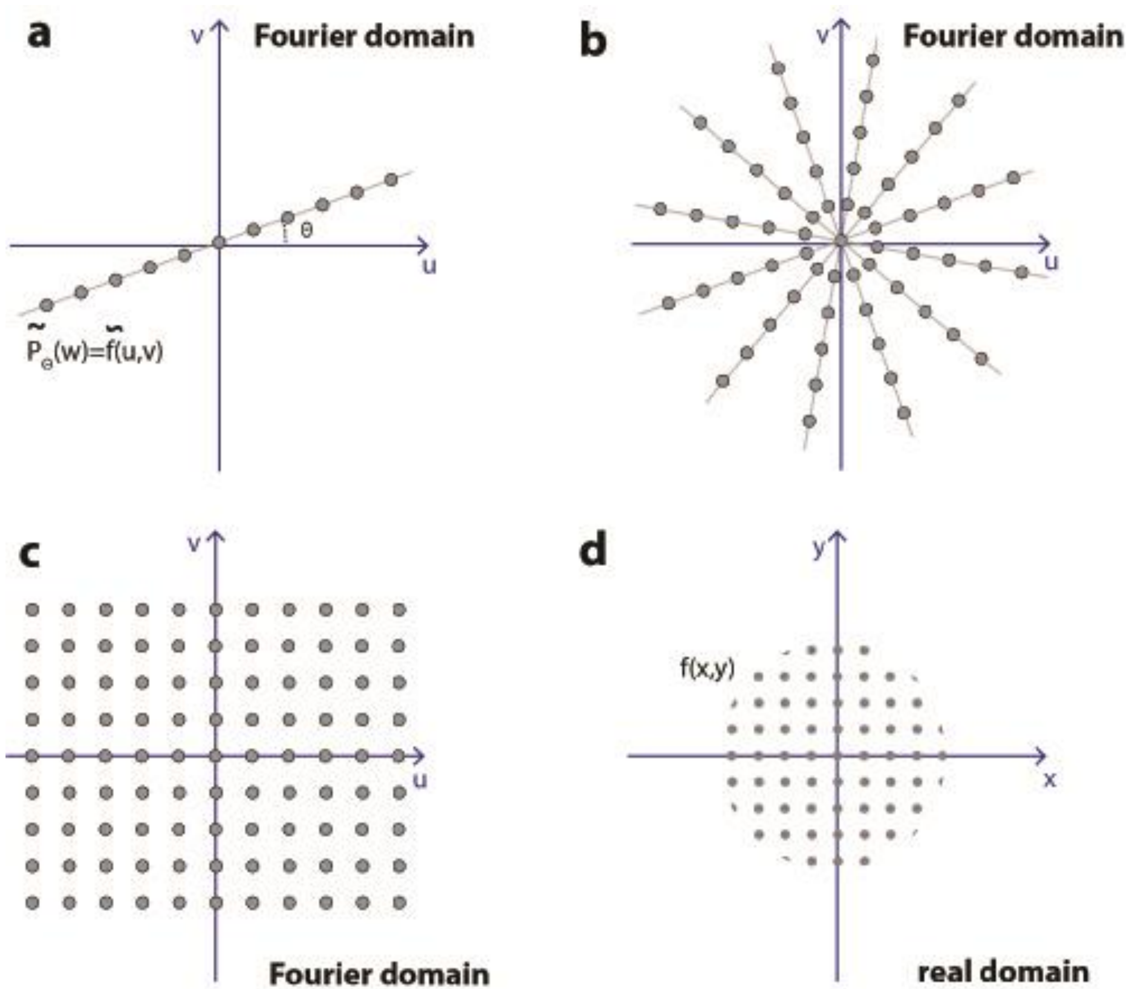

Principle for tomographic reconstruction

1. Collect projections, $P_\theta(x')$, for several angles
2. Calculate the Fourier transform of each projection
3. Apply the filter to Fourier domain to approximate the ideal case
4. Find the inverse Fourier transformation of the filtered projection
5. Sum over all angles to make the reconstruction

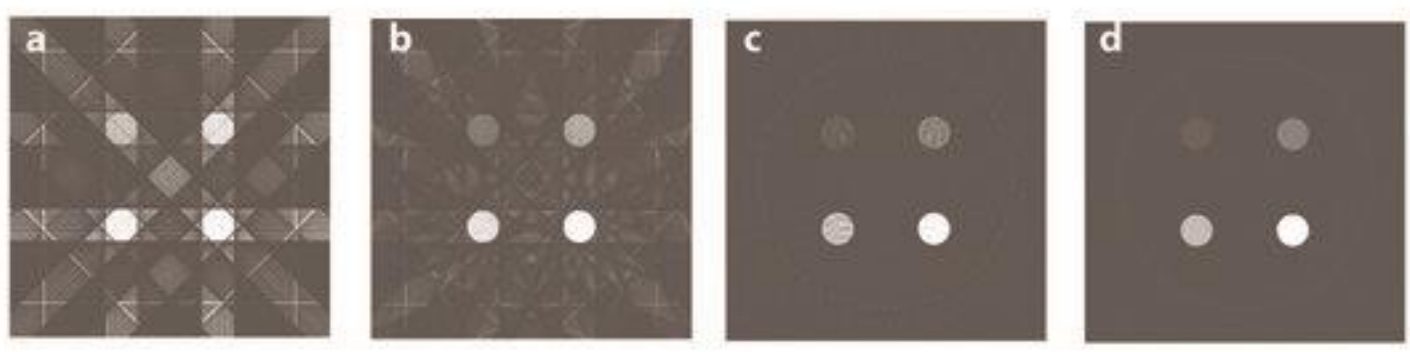

4 projections 8 projections 32 projections 128 projections

Cases:
Proton Exchange Membrane Fuel Cell (PEMFC)

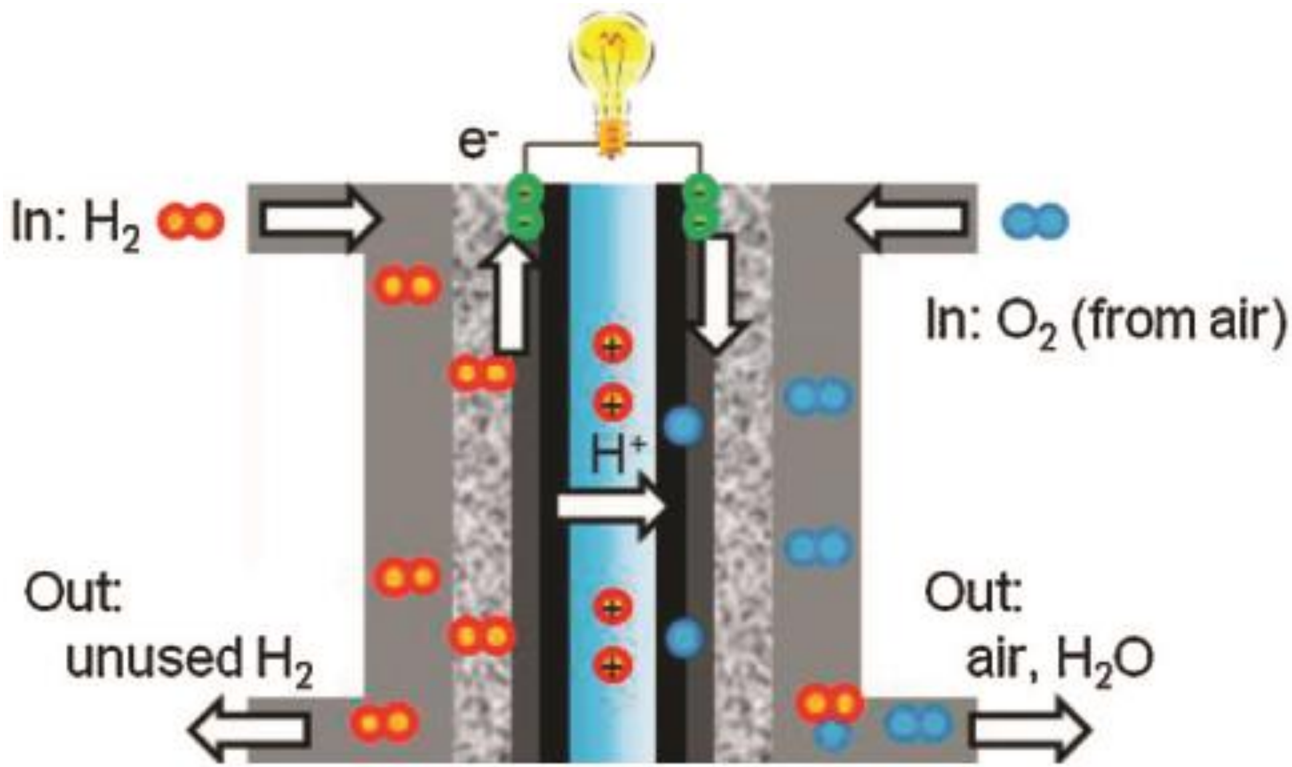

Mischler, J. et al. (2010). *Electrochimica Acta.* **75**, 1.

Cases:
in situ study of water in PEMFC

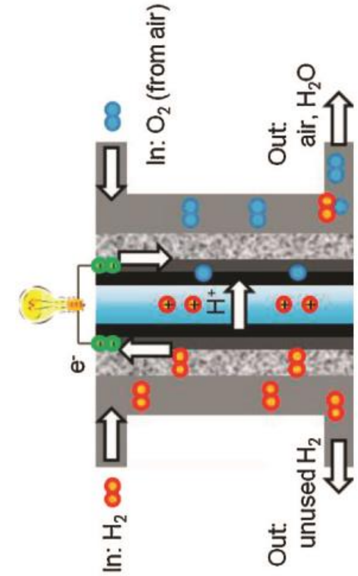

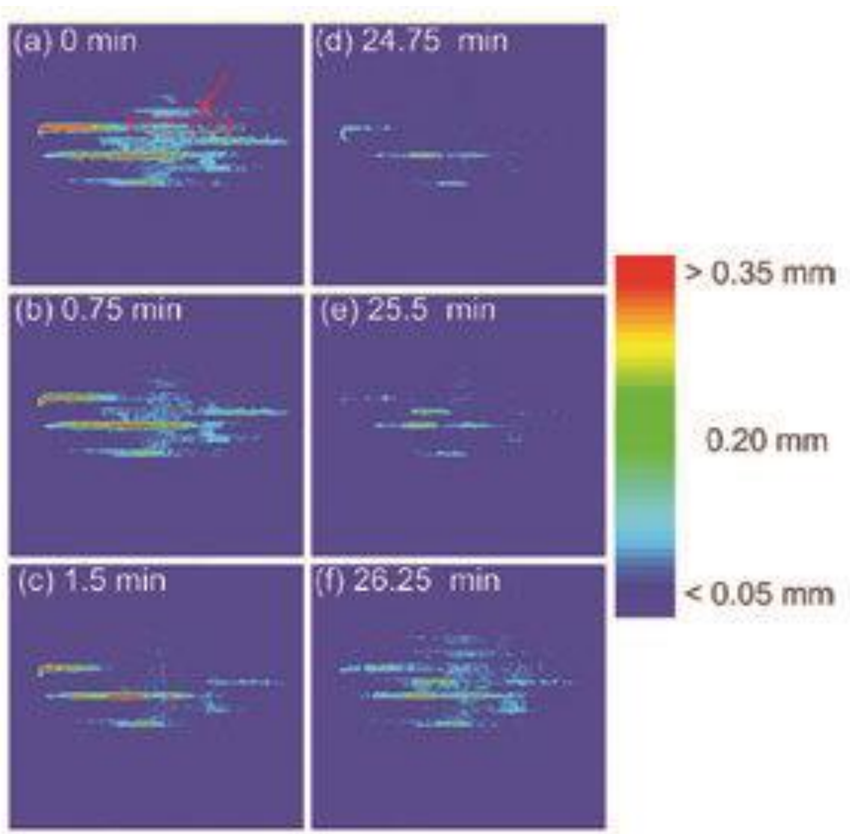

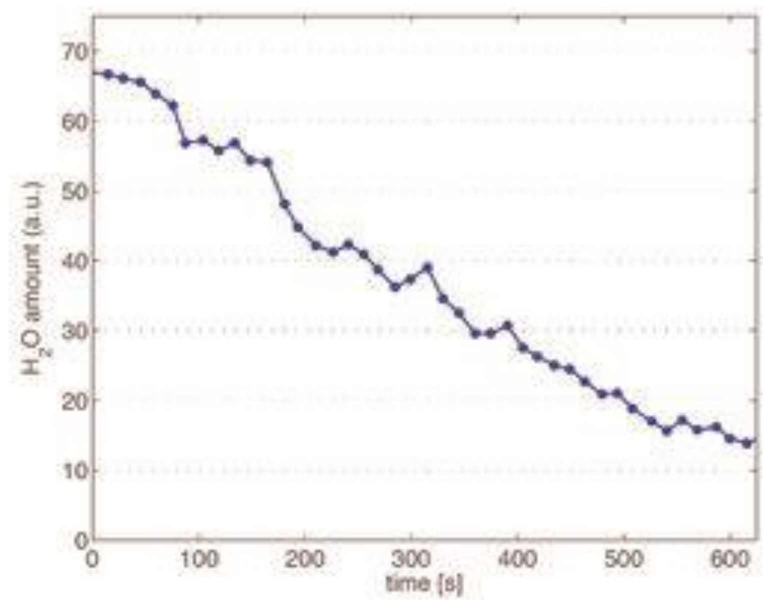

Manke, I. et al. (2009). *Appl. Phys. Lett.* **92**, 244101.

Cases: water uptake in plants

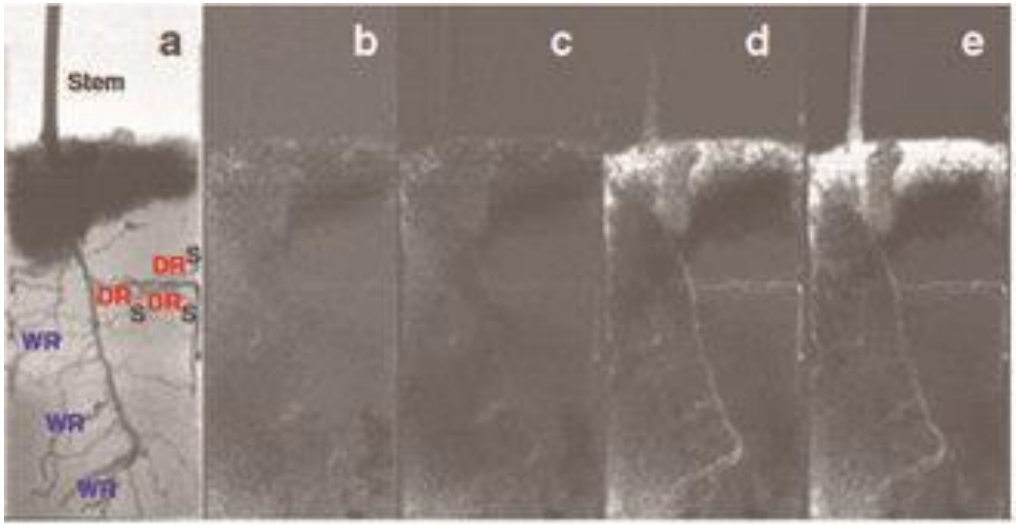

0.25h 0.5h 6h 12h

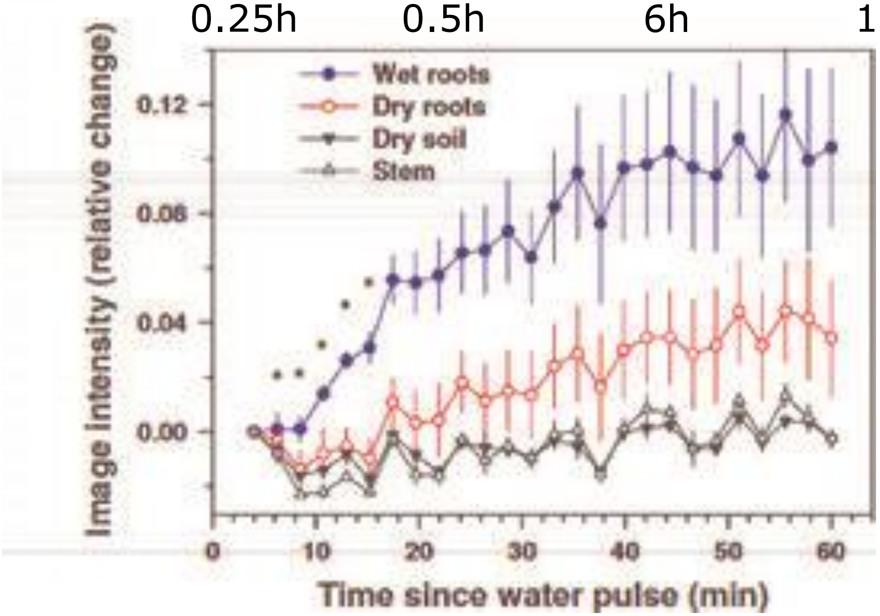

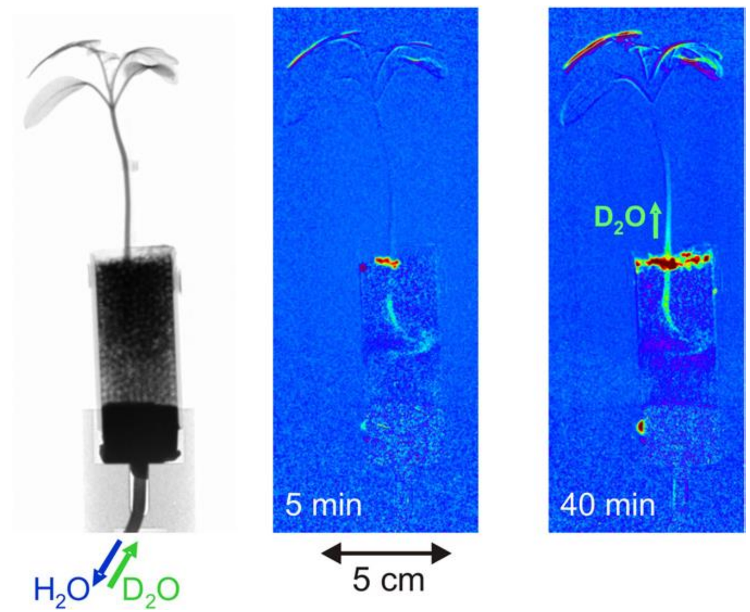

Strobl, M. et al. (2009). *J. Phys. D. Appl. Phys.* **42**, 243001.

Cases:
Alkaline battery   Li-air battery cathode

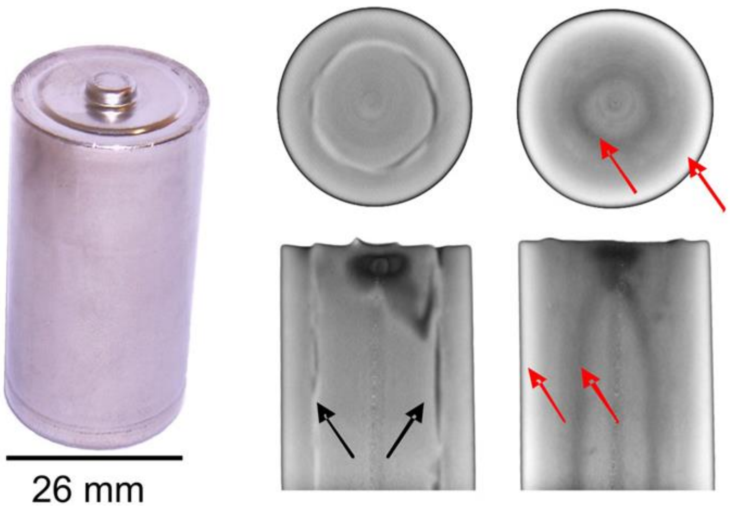

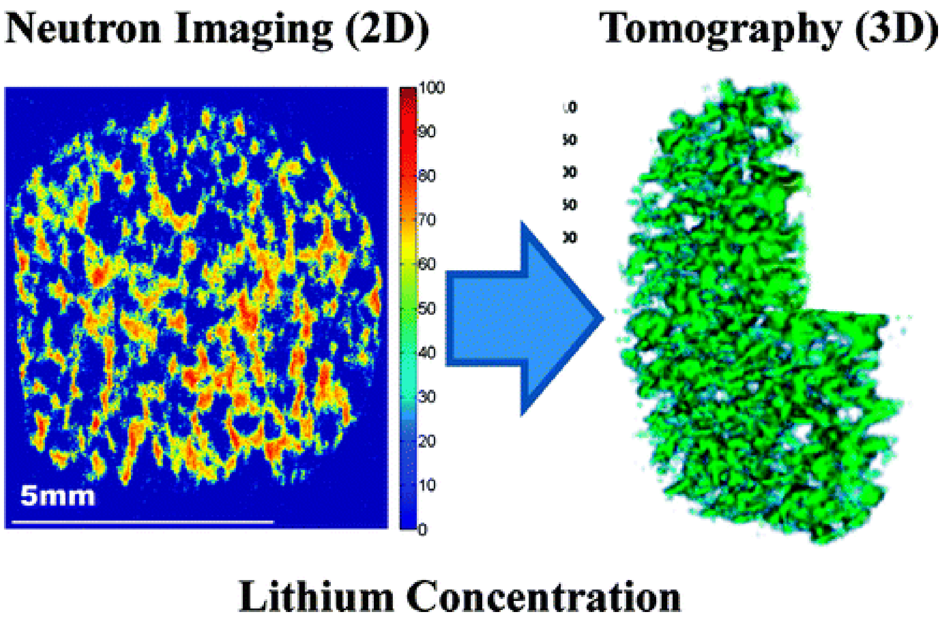

Strobl, M. et al. (2009). *J. Phys. D. Appl. Phys.* **42**, 243001.

Nanda, J. et al. (2012). *J. Phys. Chem. C.* **116**, 8401.

Cases:
Soot in particulate filter for diesel engine

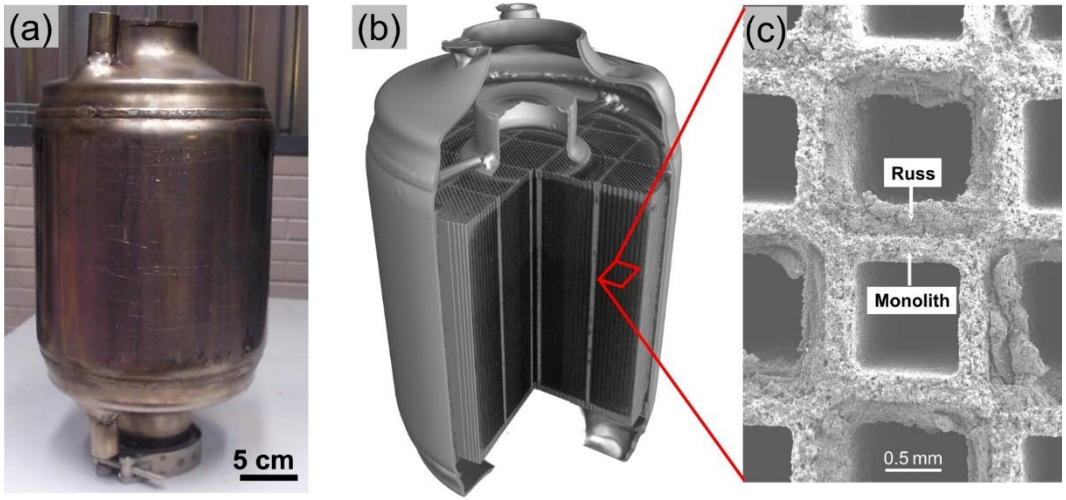

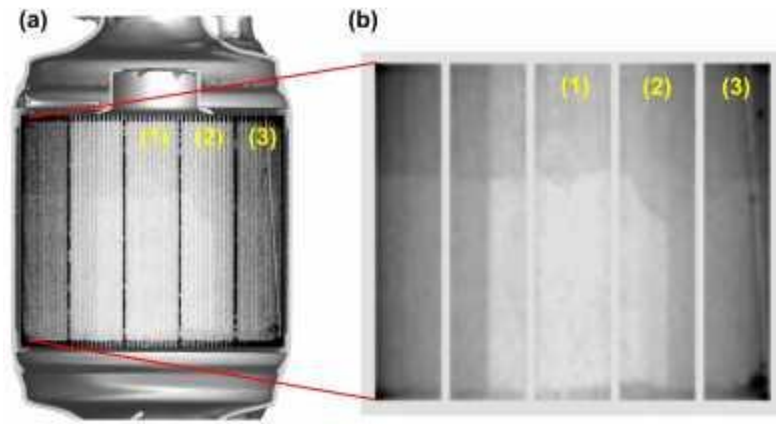

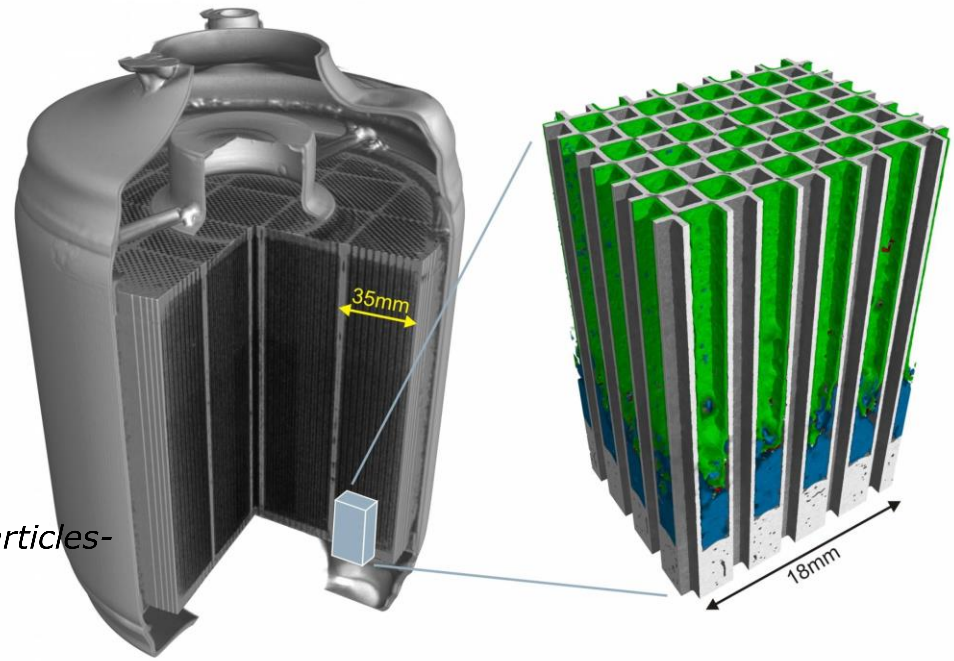

https://www.psi.ch/media/distribution-of-soot-particles-in-particulate-filters-of-diesel-vehicles

Cases: Cultural heritage

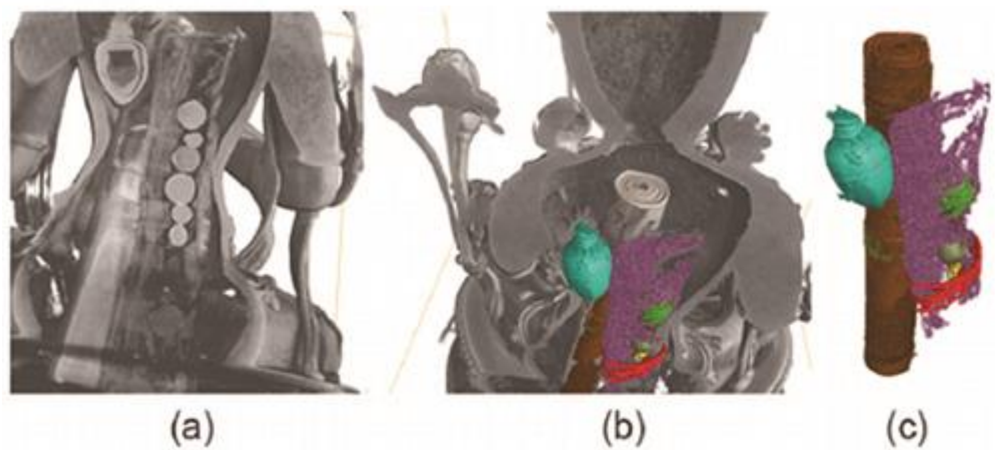

Energy-resolved neutron imaging
Bragg-edge imaging

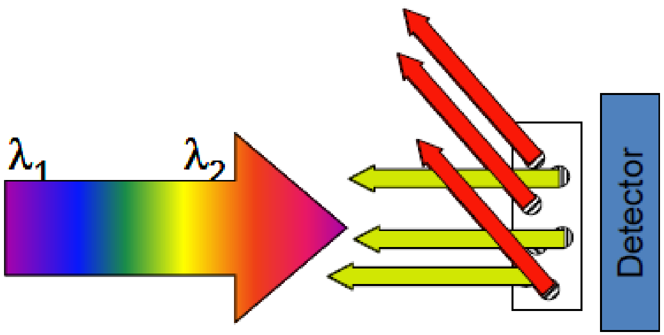

Total neutron cross section for different polycrystalline materials

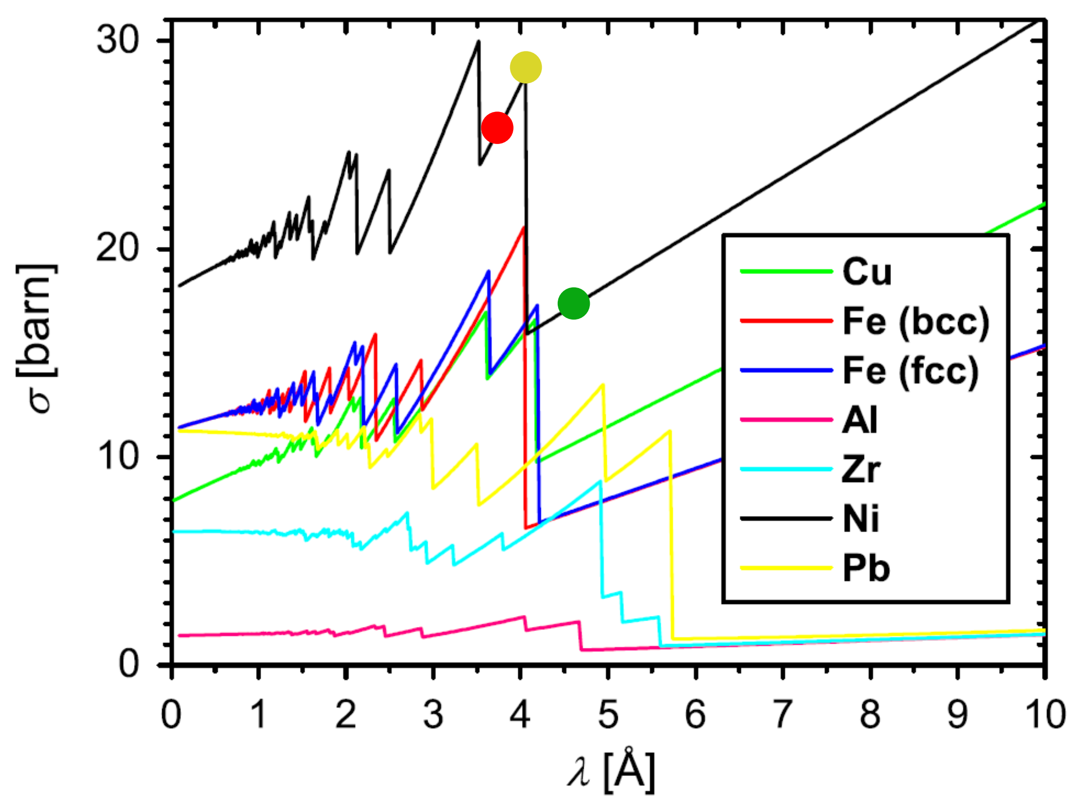

Bragg's law:

$2d_{hkl}\sin\theta = \lambda$

$2d_{hkl}\sin 90^\circ = \lambda$

$2d_{hkl}\sin\theta < \lambda$

Josic, L. et al (2011). *Nucl. Instruments Methods Phys. Res.* **651**, 166.

Energy-selective neutron imaging
Case: welding of steel

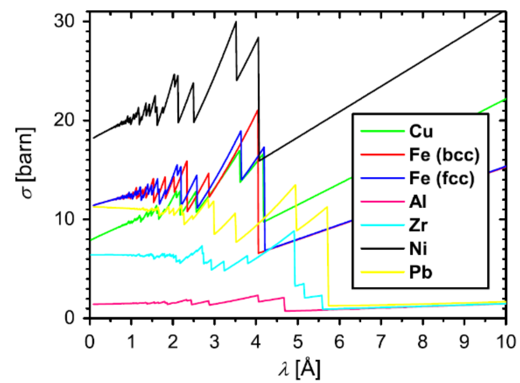

3.4 Å

4.0 Å

4.4 Å

In situ Bragg-edge imaging linking strain and reduction in Solid Oxide Cell electrode supports

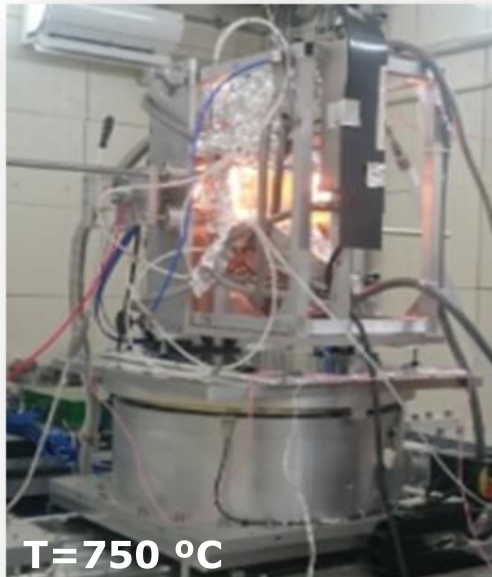

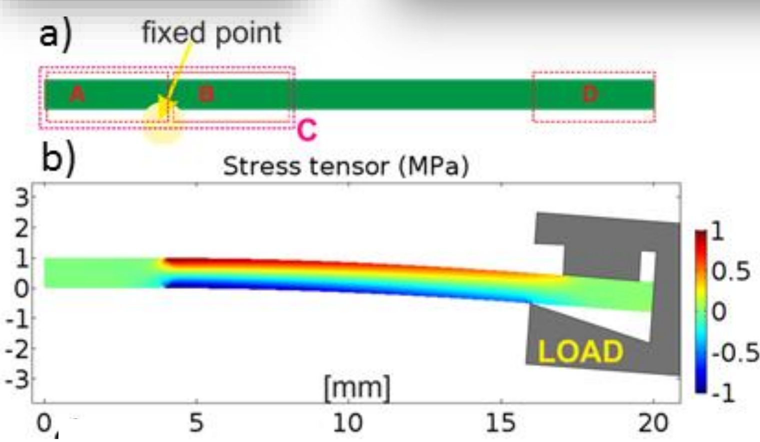

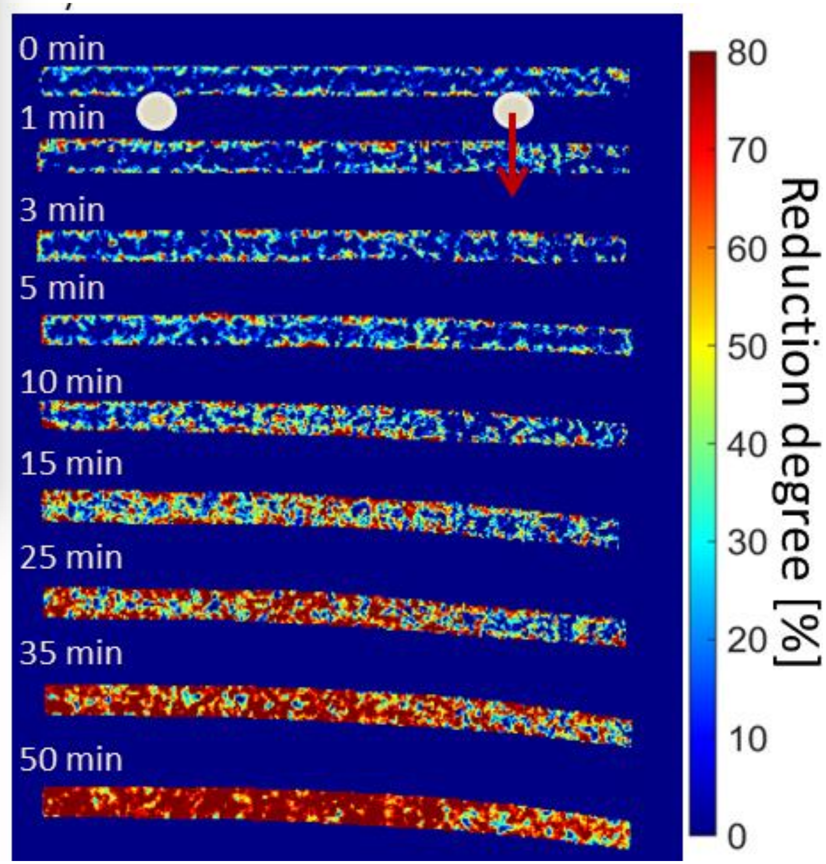

M. Makowska et al, J.Appl.Cryst. ***48****, 401(2015)*

M. Makowska et al, J. Appl. Cryst. ***49****, 1674 (2016)*

Neutron Bragg-edge tomography of crack evolution after 5x red-ox cycling

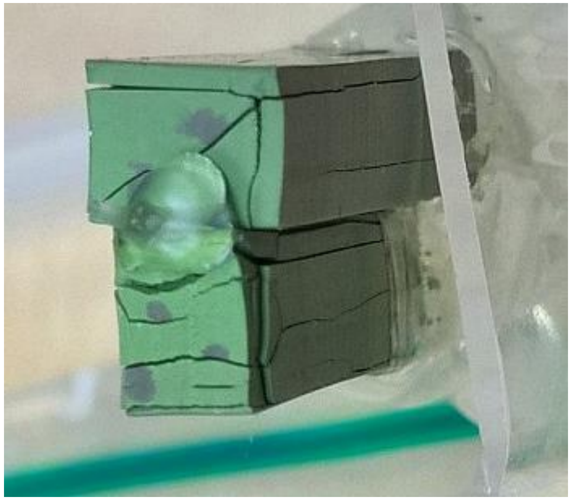

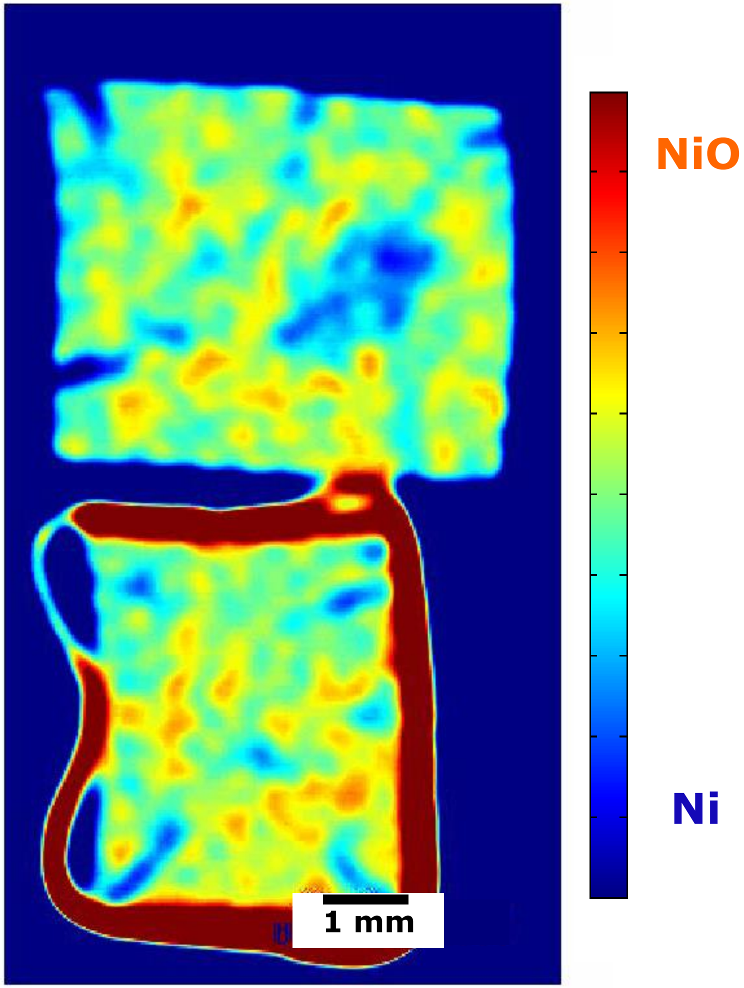

M. Makowska et al, submitted (2017)

Neutron grating interferometry

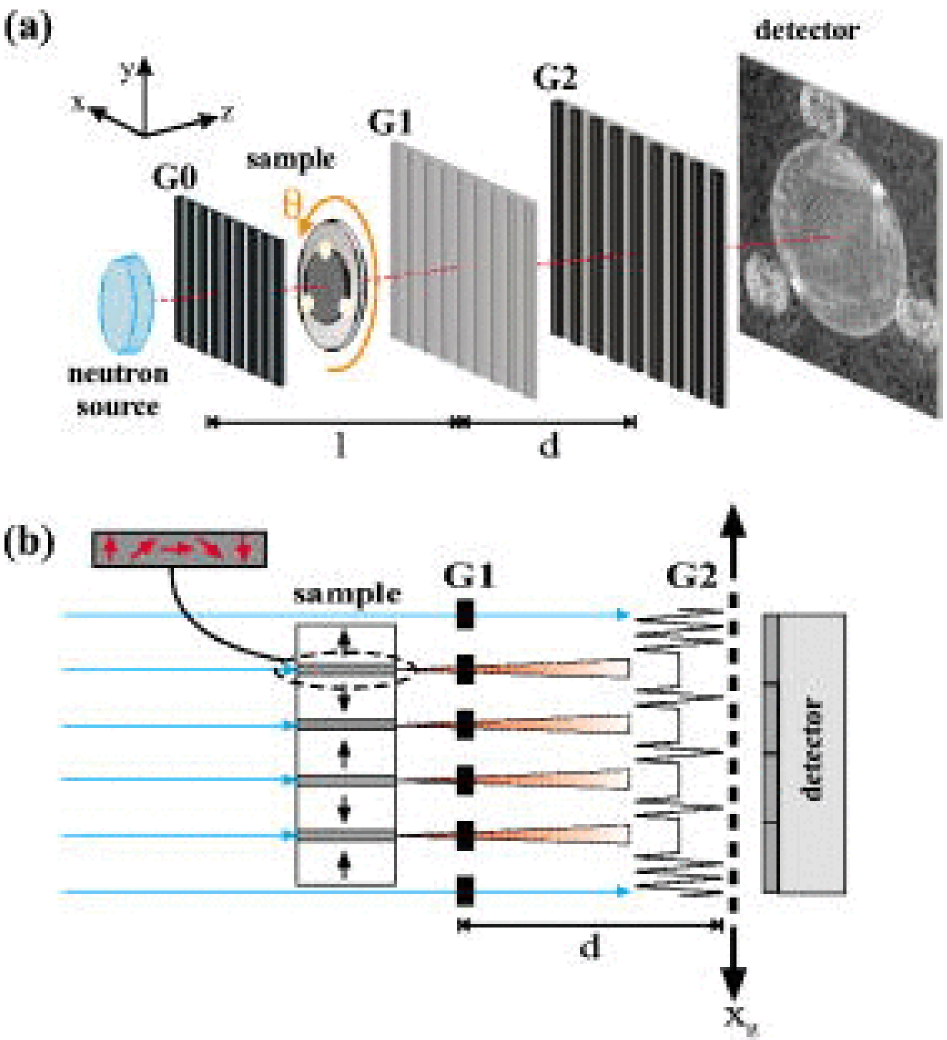

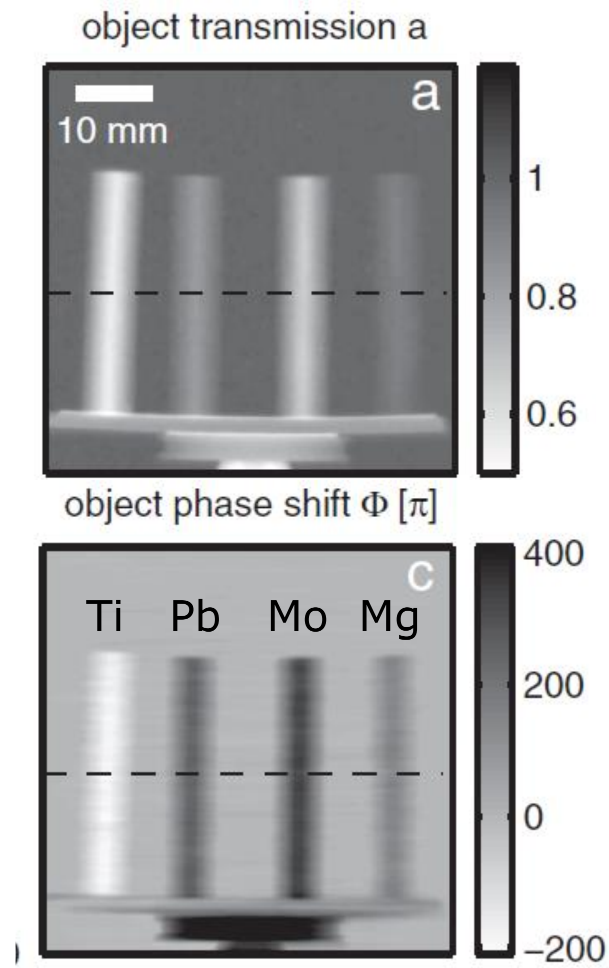

Grünzweig, C. et al. (2006). *Phys. Rev. Lett.* **96**, 215505.
Grünzweig, C. et al. (2008). *Appl. Phys. Lett.* **93**, 112504.

3D polarimetric neutron tomography of magnetic fields and current distributions

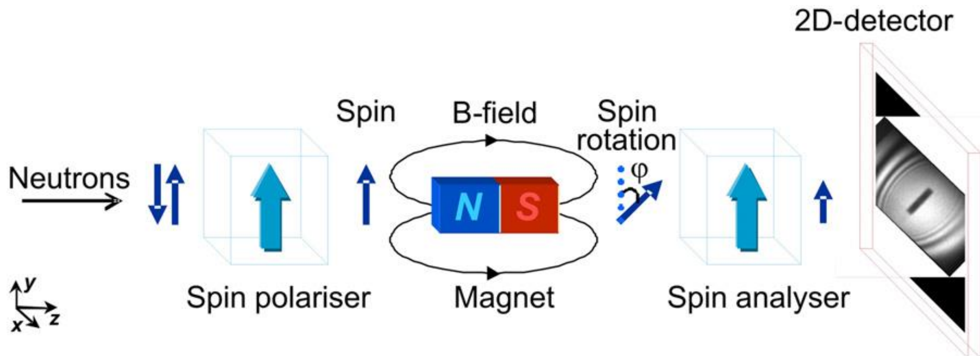

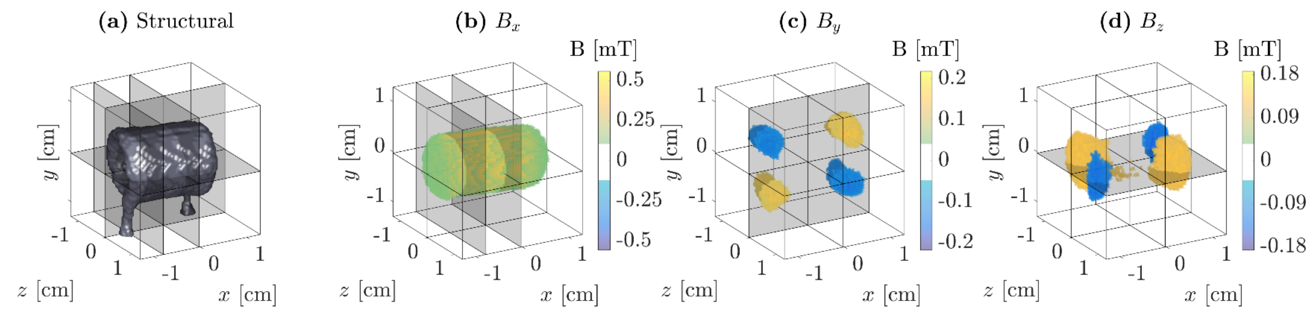

M. Sales et al, submitted (2017)

Summary

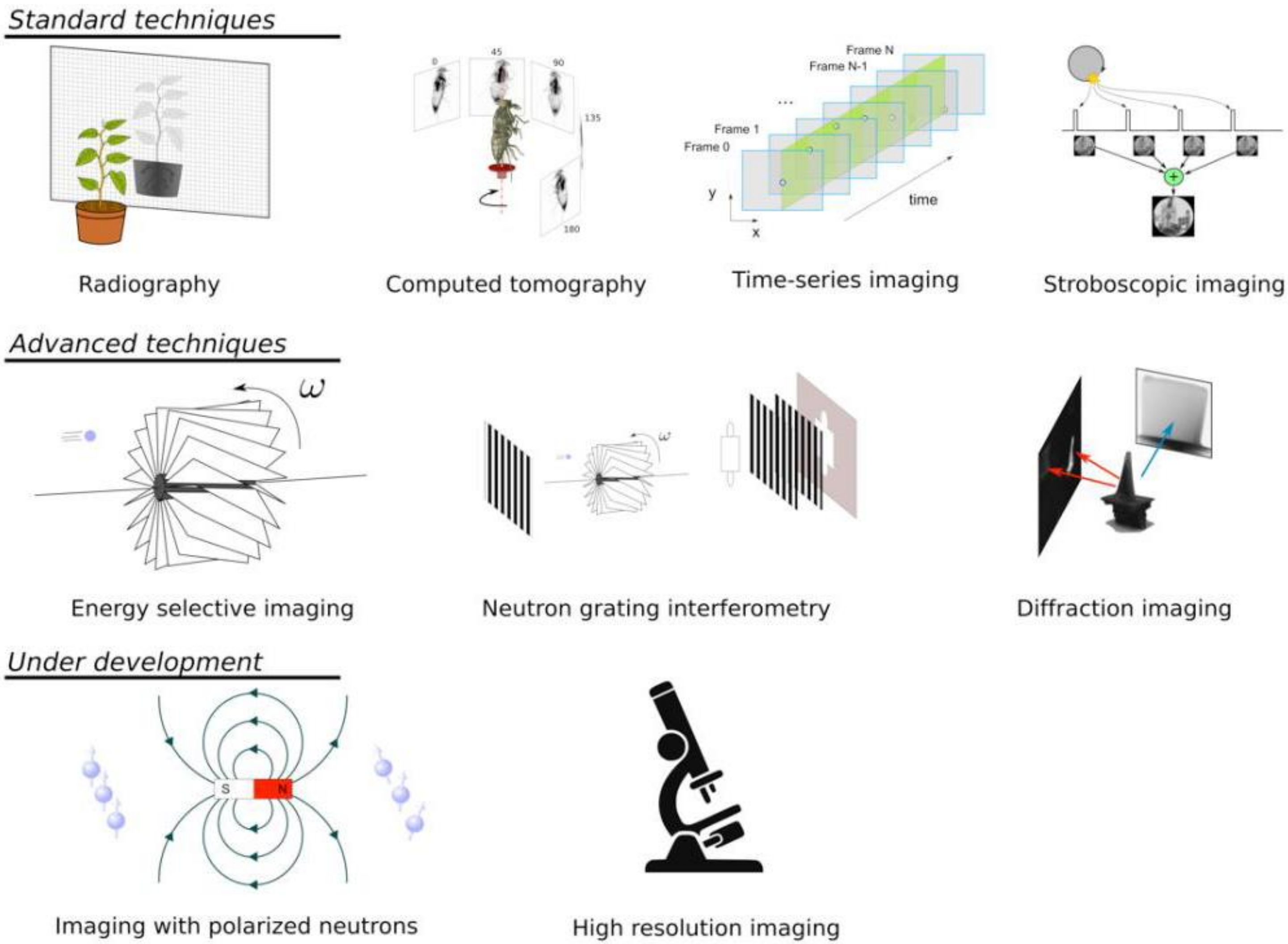

Lehmann, E. et al. (2017). *Phys. Proc.* **88**, 5.

Acknowledgments

DTU Energy
Department of Energy Conversion and Storage

M. Makowska (now FRM II, Münich), M. Lacatusu,
H. Lund Frandsen, L. Nilausen Cleemann
S. Koch, J. Johnsen

DanScatt

DTU

xnovotech

E. Mejdal Lauridsen

DTU Physics
Department of Physics

S. Schmidt, M. Sales

J-PARC

Takenao Shinohara

European Union
European Regional
Development Fund

The Czech Academy of Sciences

Petr Sittner

PAUL SCHERRER INSTITUT
PSI

M. Strobl
M. Morgano

HZB Helmholtz Zentrum Berlin

R. Woracek, N. Kardjilov

ess

R. Woracek

Science & Technology Facilities Council
ISIS

S. Kabra, W. Kockelmann

SPACE SCIENCES LABORATORY
Berkeley

A. Tremsin

Interreg
EUROPEAN UNION
Öresund-Kattegat-Skagerrak
ESS & MAX IV: Cross Border Science and Society
This project is sponsored by the European Regional Development Fund

NordForsk

In situ Bragg-edge imaging of red-ox cycling (750 ºC) of Solid Oxide Cell electrode supports

Initial oxidized state | After reduction | After oxidation | After reduction | After oxidation

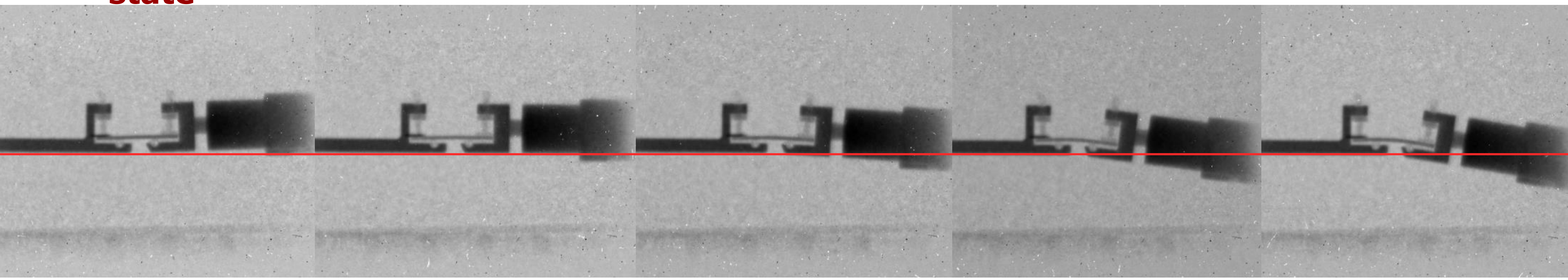

Initial oxidized state

20 mm

Reduced

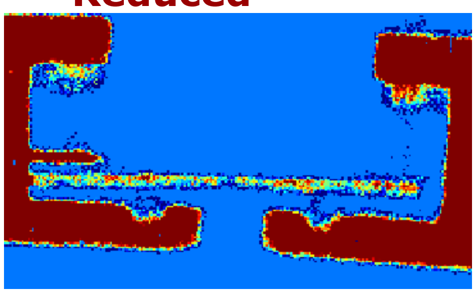

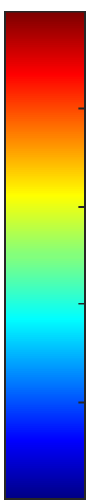

Macroscopic cross section [1/mm]

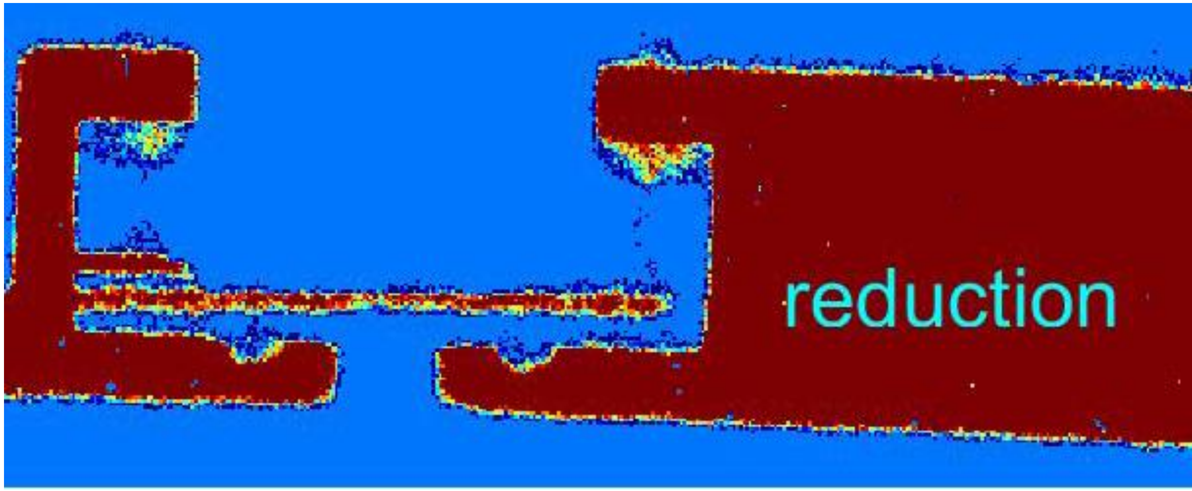

M. Makowska et al, *J. Power Sources* **340**, *167 (2017)*